Chapter 13
Detection of Biosignatures Using Raman Spectroscopy

Frédéric Foucher

Abstract Raman spectroscopy is particularly suited for the study of biosignatures: it is able to detect both organic and mineral phases, is very sensitive to carbonaceous matter and biogenic pigments, and can be used in the field and for space exploration. Thus, in a few decades it has become a key method in (micro-)palaeontology, geomicrobiology and astrobiology. In this chapter, we present an overview of the different types of biosignatures that can be detected and/or characterized using Raman spectroscopy: organic molecules, microfossils, biominerals or even living cells. A particular focus is made on the role of the excitation laser wavelength on the type of biosignatures that can be studied.

13.1 Introduction

The term biosignature refers to any direct or indirect evidence of active or past life. It includes living organisms and their fossils, as well as organic compounds of biological origin, biominerals and biogases produced by metabolic activity, or physical structures created by living organisms, such as shells or stromatolites. The detection of biosignatures is of primary importance for micropalaeontology to demonstrate the biogenicity of a fossilized structure and for astrobiology, where the objective is the search for past or present extraterrestrial life. Detection of biosignatures involves the use of a large range of techniques and instruments to make observations, determine elementary and molecular composition, date the structures, and characterise the geochemical environment.

Raman spectroscopy is a versatile technique that uses a laser to detect and identify molecules and crystals. In the laboratory, the instrument can be equipped with a scanning device permitting it to display composition over a selected area of analysis. Raman instruments generally use optical microscope objectives and are confocal in order to carry out compositional mapping in 2D and 3D, from the centimetre to

F. Foucher (✉)
Centre de Biophysique Moléculaire-CBM, CNRS, Orléans, France
e-mail: frederic.foucher@cnrs.fr

B. Cavalazzi, F. Westall (eds.), *Biosignatures for Astrobiology*, Advances in Astrobiology and Biogeophysics, https://doi.org/10.1007/978-3-319-96175-0_13

sub-micrometre scale (Deing et al. 2010; Foucher et al. 2017). Miniaturized, it can be used for field investigation and planetary exploration (Culka et al. 2011, 2012; Edwards et al. 2013). It will be a key instrument during the future missions to Mars *ExoMars 2020* (ESA-Roscosmos), with the *Raman Laser Spectrometer*, *RLS*, (Rull-Pérez and Martinez-Frias 2006; Lopez-Reyes et al. 2013), and *Mars 2020* (NASA), with *SHERLOC* (for *Scanning Habitable Environments with Raman & Luminescence for Organics & Chemicals*) and *SuperCam* (Beegle et al. 2014).

Raman spectroscopy is well suited for studying biosignatures but, depending on the system used (field or laboratory instrument) and on the excitation laser wavelength, the types of biosignatures that can be detected may vary. In particular, luminescence of the sample may mask the Raman signal, the laser may heat and alter the sample, or the embedding phase (e.g. the mineral matrix) may be opaque at certain wavelengths.

In this chapter, the Raman effect is explained first. In particular, the focus is placed on the advantages and disadvantages of the different laser wavelengths from deep ultra violet (UV) to infrared (IR) on instrumentation and biosignature detection. The different types of biosignatures that can be detected using Raman spectroscopy are then described, from biominerals to living organisms.

13.2 Raman Effect and Instrumentation

The Raman effect was described for the first time by Chandrasekhara Venkata Rāman in 1928. It corresponds to the inelastic scattering of photons leading to atomic bond vibrations. This phenomenon requires advanced physics to be fully described, thus, this chapter will only briefly explain the effect. However, full descriptions can be found in several books such as Poilblanc and Crasnier (2006), Deing et al. (2010) or Dubessy et al. (2012).

Photons in the UV to IR range of the electromagnetic spectrum may transfer energy to molecules or crystals as vibrations or as electronic transitions, depending on their energy (see Fig. 13.1).

The vibrational energy transitions involved in the Raman effect are in the order of magnitude of a few tenths of eV, while the energy between the excited electronic states and the ground electronic state is generally of about ~2 eV. According to the Planck-Einstein equation,[1] it is easy to convert wavelength into energy. Thus, IR electromagnetic radiation extending from 700 nm to 1 mm corresponds to photon energies ranging from 1.77 to 0.001 eV, respectively (i.e. from 10 to 15,000 cm^{-1}). Photons in the range 0.06–0.5 eV (i.e. 2.5–20 μm or 500–4000 cm^{-1}) may then be absorbed by inducing ground electronic vibrational state transitions. This phenomenon is used for IR spectroscopy. In the visible range, from 400 to 700 nm (1.77–3.10 eV respectively), a

[1]The Planck-Einstein equation is given by $E = h.c/\lambda$ with E the energy, h the Plank constant, c the speed of light in vacuum, and λ the wavelength.

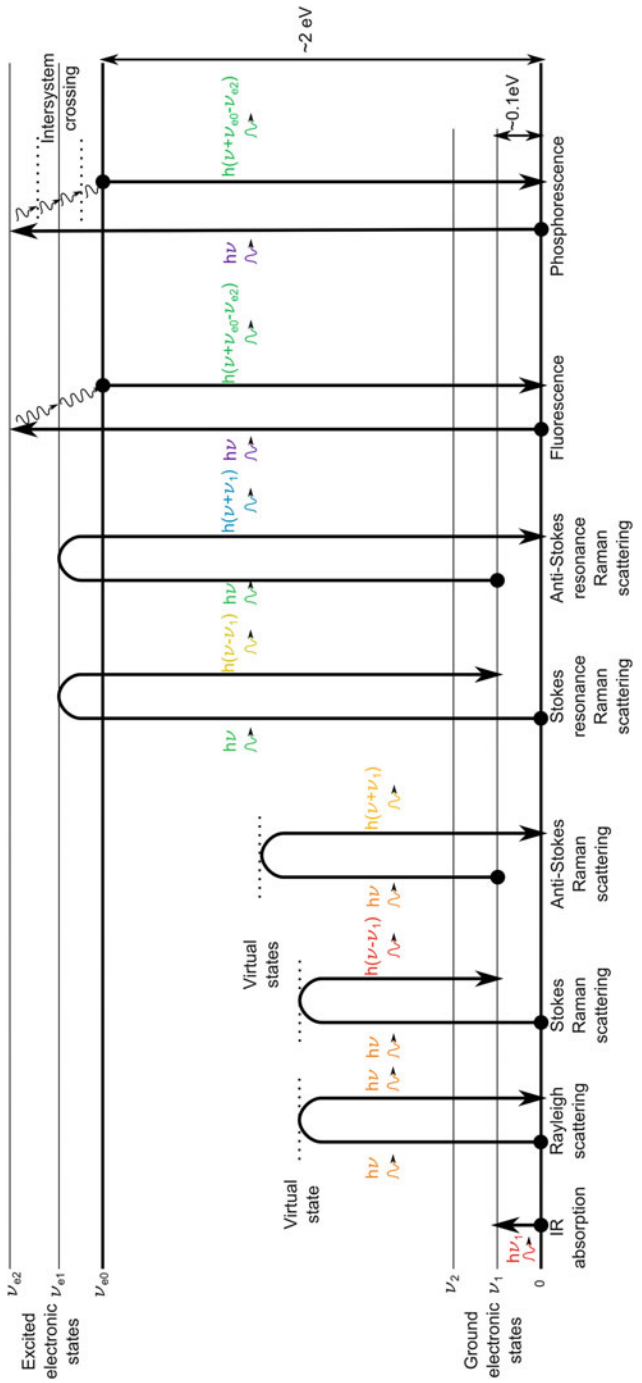

Fig. 13.1 Non-exhaustive possible photon-matter interactions in the IR to UV range of the electromagnetic spectrum. Source: F Foucher

photon could either be elastically scattered (Rayleigh effect), i.e. scattered with no loss of energy, or inelastically scattered (Raman effect), i.e. scattered with change of energy. If the photon loses energy, it undergoes Stokes Raman scattering and, on the contrary, if the photon gains energy (which is less probable), it undergoes Anti-Stokes Raman scattering. With decreasing wavelength, from about 200 to 550 nm (6.2–2.25 eV respectively), the energies of the photons are in the order of magnitude of those of excited electronic states. This may then lead to luminescence (fluorescence and phosphorescence) and resonance Raman (RR) scattering.

Fluorescence occurs when molecules reach an excited electronic state by absorbing the incident photons, de-exciting progressively by non-radiative transitions, and finally returning to the electronic ground state by emitting photons of lower energy (i.e. higher wavelength). The phosphorescent effect is similar but slower due to intersystem crossing. Finally, RR scattering occurs when the energy of the incident photons is close to an electronic transition of particular atomic bonds leading then to a resonant effect (i.e. an increase in probability of occurrence of Raman scattering). RR is characterized by strong enhancement of the intensity of certain bands of the Raman signal (by several orders of magnitude). Raman scattering is very short (~ns) in comparison with fluorescence (~μs to ms) and phosphorescence (~s to min) where the photons are absorbed and re-emitted. Raman intensity is also very weak compared to luminescence but the RR signal can be of the same order of magnitude or even higher.

The Raman effect is sensitive to atomic bonds. It permits the discrimination of polymorphic minerals, i.e. minerals having similar compositions but different crystalline structures. For example, anatase, rutile and brookite have different Raman signals despite their identical elemental composition (TiO_2).

Modern Raman spectroscopy is performed using a monochromatic light source (laser) to induce the effect. The scattered signal is diffracted using various gratings and collected using a CCD camera interfaced with the spectrometer. The collected signal consists of a spectrum displaying the number of scattered photons *versus* their wavenumber, i.e. the shift in cm^{-1} with respect to the incident beam, the excitation laser wavelength corresponding to 0 cm^{-1}. Identification of minerals or organic compounds is made by comparison with reference spectra found in the literature or in databases.

Raman spectra extend from 0 to 4000 cm^{-1} irrespective of laser wavelength. However, their range in wavelength increases with increasing excitation laser wavelength, as shown in Fig. 13.2a. The choice of laser is crucial depending on the target. For instance, organic molecules are known to be particularly fluorescent. A deep UV laser at 250 nm appears therefore to be a good solution, the Raman spectra being collected before the beginning of luminescence (Fig. 13.2a). Moreover, a short wavelength will favour the RR effect. However, in addition to being expensive and difficult to implement, UV Raman spectroscopy is limited by the depth of penetration of UV which is generally very small in solids (only a few nm), and by the possibility of burning the sample. On the other hand, the IR laser permits collection of the signal

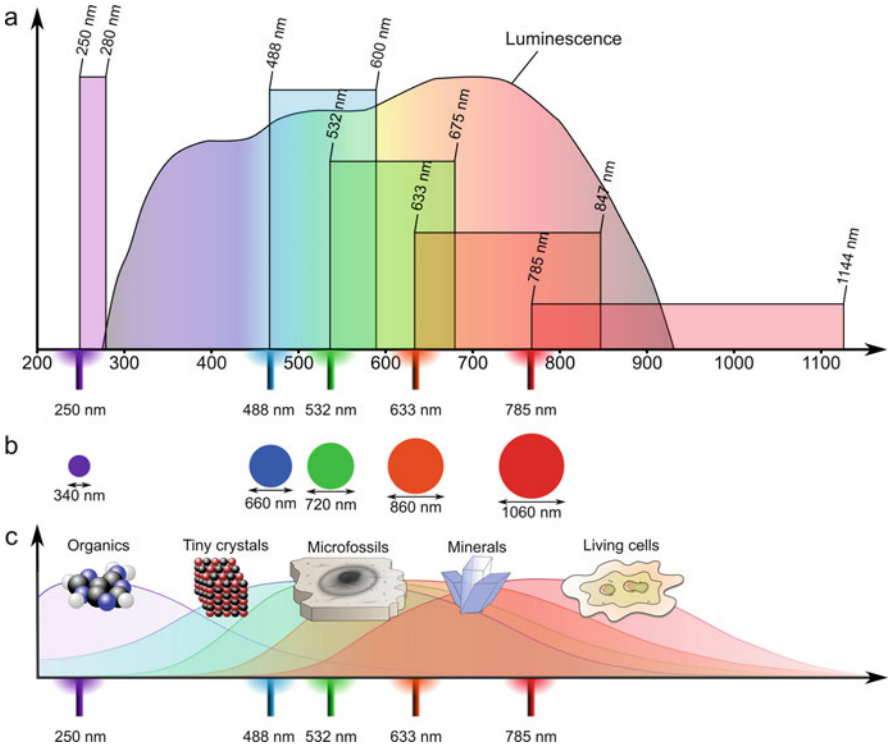

Fig. 13.2 (**a**) General luminescence envelope and Raman spectrum ranges (corresponding to 0–4000 cm^{-1}) for different excitation laser wavelengths (adapted from Beegle et al. 2014). (**b**) Laser spot size through an objective of numerical aperture 0.9. (**c**) Suitability of the different laser wavelengths to be used to study biosignatures. Source: Adapted from Beegle et al. (2014)

after the fluorescence range (Fig. 13.2a) with less risk of burning the sample. However, CCD detectors are less sensitive in the IR range and therefore the Raman signal is less intense, particularly after 900 nm (the use of 1064 nm IR excitation laser requires the use of FT-Raman systems). In order to compensate for this low signal gain it may sometimes be necessary to use high laser power, thus, increasing the risk of burning the sample. Moreover, following the Airy disk principle,[2] the laser spot diameter increases with the wavelength (Fig. 13.2b).

Finally, the depths of field and of penetration are also increased in such a way that the analysed volume may then be relatively large (several μm^3) thus requiring a larger amount of material in order to be detected.[3]

[2]The Airy disk corresponds to the best focused spot of light through an optical system. Its diameter is given by $D = 1{,}22.\lambda/NA$, with NA the numerical aperture of the objective.

[3]The depth of field of an objective is given by $\Delta z = n.\lambda/(2.NA^2)$, with n the refractive index of the material.

To summarise, a UV laser is well suited for the detection of organic molecules adsorbed on the surface and to carry out high-resolution surface analyses. An IR laser allows performing Raman at depth with less risk of burning; it is thus well suited for living tissues, for instance. In between, the available lasers are good compromises and are particularly suitable for studies of carbonaceous microfossils in a mineral matrix. The *ExoMars 2020 RLS* and the *Mars 2020 SuperCam* Raman systems will thus be equipped with a green laser (wavelength of 532 nm). Figure 13.2c shows the suitability of the different laser wavelengths for studying biosignatures.

Portable instruments for field investigations generally use optical fibres or macroscopic lenses. Their spatial resolution is, consequently, most of the time relatively low with a spot size of several tens of micrometres to millimetres (Mosier-Boss and Putnam 2013). The miniaturization of the systems also leads to a decrease in spectral resolution (several cm^{-1}) (Culka et al. 2011, 2012; Vitek et al. 2012). For practical reasons they generally use high laser wavelength, from 532 to 1064 nm (Vitek et al. 2012). By contrast, most laboratory systems are based on an optical microscope architecture, which allows significant increase in the resolution of analyses and, when interfaced with a scanning system, to carry out mapping. A Raman map is made by scanning an area of interest with the laser while accumulating spectra. By attributing a colour scale to the Raman signal intensity of a given compound, it is then possible to display its concentration through the chosen area. It is also possible to attribute a different colour to each compound in order to obtain a compositional map. More information on mapping technique can be found in Deing et al. (2010) or Foucher et al. (2017). Finally, instruments for space exploration can be seen as intermediate systems in terms of spatial and spectral resolution and in terms of capacities (quite good resolution but no mapping, for instance).

13.3 Biosignatures Raman Detection

13.3.1 Organic Molecules

Astrobiology mainly focusses the search for life on auto-replicating systems capable of Darwinian evolution and based on organic chemistry in liquid water (Lazcano 2011; Ruiz-Mirazo and Moreno 2011). All known living systems on Earth are indeed more than 95% based on the elements C, H, N, O, P and S, and this chemistry appears to be the only way to form enough various and complex molecules to enable life to appear and evolve (Brack 2001).

Organic molecules can be identified by Raman spectroscopy and various spectral databases are available. Examples of typical spectra of organic molecules are displayed in Fig. 13.3 (De Gelder et al. 2007).

A large variety of organic molecules have been found in the interstellar medium (Dickens et al. 2001), icy dust particles (Danger et al. 2013; de Marcellus et al. 2015; Meinert et al. 2016), comets (Altwegg et al. 2016) and meteorites (Schmitt-Kopplin

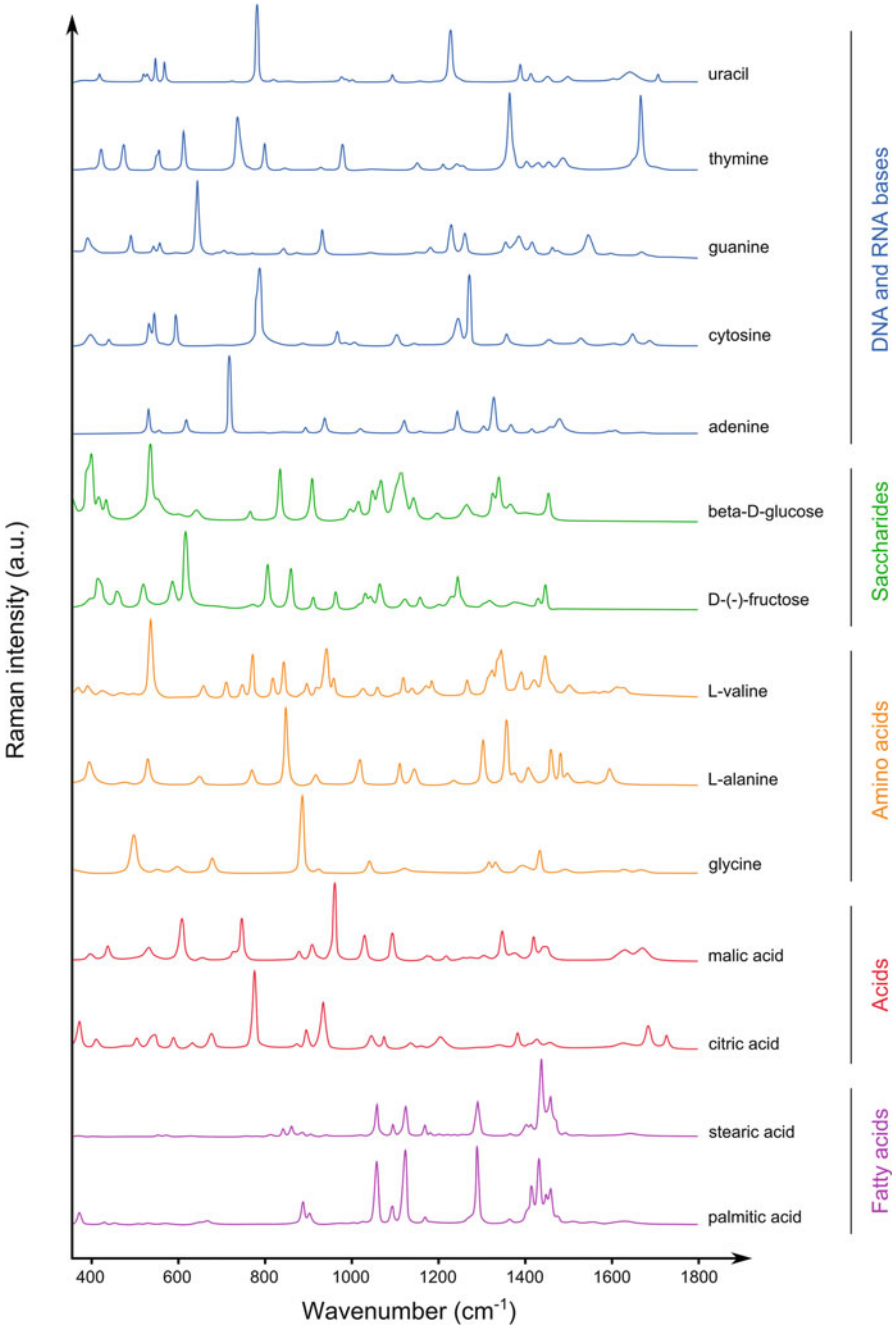

Fig. 13.3 Raman spectra of some biological molecules acquired on pure compounds using a 785 nm excitation laser wavelength. Source: Adapted De Gelder et al. (2007)

et al. 2010) demonstrating that they can be abiotically synthesised. Life uses a more restricted range of organic molecules, some of which are considered as uncontroversial evidence of life, such as DNA, RNA, and proteins. NASA thus took up the challenge to send a Raman system dedicated to the search for organics on Mars during the *Mars2020* mission: the *SHERLOC* instrument. The system will use a deep UV laser permitting it to obtain (resonant) Raman spectra below the fluorescence wavelength range (see Sect. 13.2), as well as make luminescence analysis in the visible wavelength range (Beegle et al. 2014).

13.3.2 Pigments

A particular focus will be made here on pigments. Pigments are molecules that contain at least one chromophore in their structure, i.e. a chain of alternative single and double carbon bonds. By selecting the excitation laser wavelength in order to excite the π-π* electronic transition energy range in conjugated chromophores, such as those of β-carotene, or the charge transfer transition energy in metal complex chromophores, such as in chlorophyll, it is possible to strongly enhance the Raman signal by the resonance effect (RR) of the stretching modes of the π-bonds, or of the stretching modes of the metal-ligand respectively (Merlin 1985). Among these molecules, carotenoids are those associated with the strongest RR effect when a green excitation laser is employed. The signal is still strong enough to be detected out of resonance using a 785 nm excitation laser wavelength (Merlin 1985; Jehlička et al. 2009; Vitek et al. 2009).

The RR spectrum of β-carotene is displayed in Fig. 13.4. Carotenoids are relatively common biological pigments. They act as DNA-repair agents in radiation-damaged cells, protect against UV radiation and absorb light energy used for photosynthesis (Patel et al. 2004). They are found in many organisms, such as plants, algae, bacteria and archaea. The signal of carotenoids is thus commonly observed in the field using portable instrumentation. This explains why Raman studies focussed on the detection of these molecules on Mars are numerous (e.g., Edwards et al. 2013; Baqué et al. 2016; Jehlička et al. 2016). In particular, it has been shown that β-carotene can be detected in low concentrations when mixed within a mineral matrix (Vandenabeele et al. 2012). These molecules are, thus, very interesting targets for astrobiology.

13.3.3 Carbonaceous Matter and Microfossils

Carbonaceous matter as graphite or disordered sp^2 carbon is of particular interest for Raman spectroscopy since it is always resonant, whatever the excitation laser wavelength (Ferrari 2007). The technique is thus particularly suited for the study of kerogens, i.e. insoluble organic matter of biotic origin. The typical Raman spectrum of kerogen exhibits two main bands generally labelled D, for disordered, and G, for

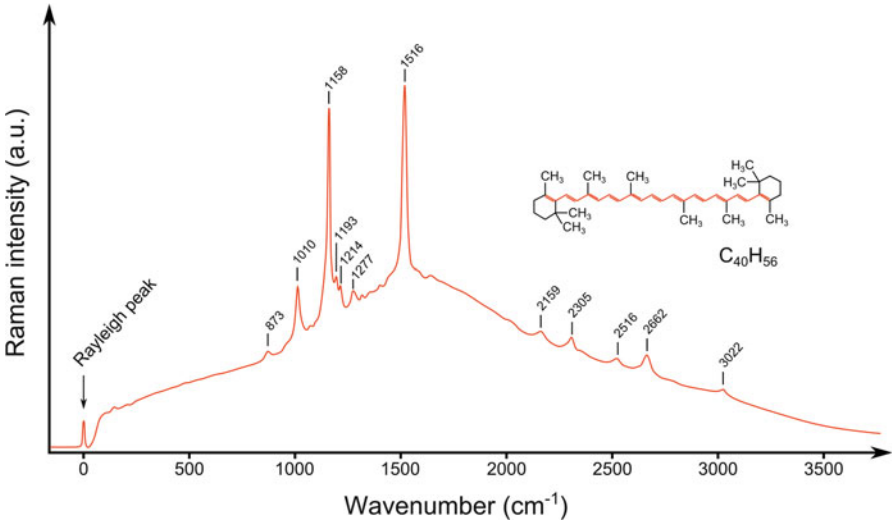

Fig. 13.4 Unprocessed Raman spectrum of pure β-carotene powder ($C_{40}H_{56}$) obtained with a 532 nm excitation laser wavelength. The RR signal is so strong that the filtered Rayleigh peak is very small in comparison and that the luminescence background is not a problem for peak detection. The chromophore is the red section in the inset molecule of β-carotene. Source: F Foucher

graphite, located respectively around ~1350 cm^{-1} and ~1600 cm^{-1} (Beyssac et al. 2002, 2003; Ferrari 2007; Foucher et al. 2015; Jehlička and Bény 1999; Jehlička et al. 2003; Lahfid et al. 2010; Quirico et al. 2009; Sforna et al. 2014). The shape of the spectrum changes with increasing metamorphism (mainly temperature) first by carbonization, then by graphitization as displayed in Fig. 13.5 (Deldicque et al. 2016; Foucher et al. 2015; Rouzaud and Oberlin 1989; Schopf et al. 2005).

Carbonization refers to the conversion of organic molecules into kerogen and is characterized by the formation of pure polyaromatic carbons forming small coherent domains. During graphitization, these coherent domains increase until, in the case of high-grade metamorphism, they form pure graphite (amphibolite facies and higher) (Bustin et al. 1995).

The Raman spectrum of kerogen was first proposed by Pflug and Jaeschke-Boyer (1979) as a tool for proving the biogenicity of carbonaceous matter in ancient sediments and then by Schopf et al. (2002a). However, spectral shapes similar to those described in these studies were observed in carbonaceous matter of abiotic origin (in meteorites, for example), thus leading to a strong debate about the origin of carbonaceous structures observed in ancient rocks (Brasier et al. 2002; Marshall et al. 2011, 2012; Marshall and Marshall 2013; Pasteris and Wopenka 2002, 2003; Schopf et al. 2002a, b). Finally, it is now acknowledged that, although the high sensitivity of Raman spectroscopy to carbonaceous matter makes it the best technique for detecting kerogens in geological samples, the shape of the Raman spectrum alone cannot be used as a proof of biogenicity.

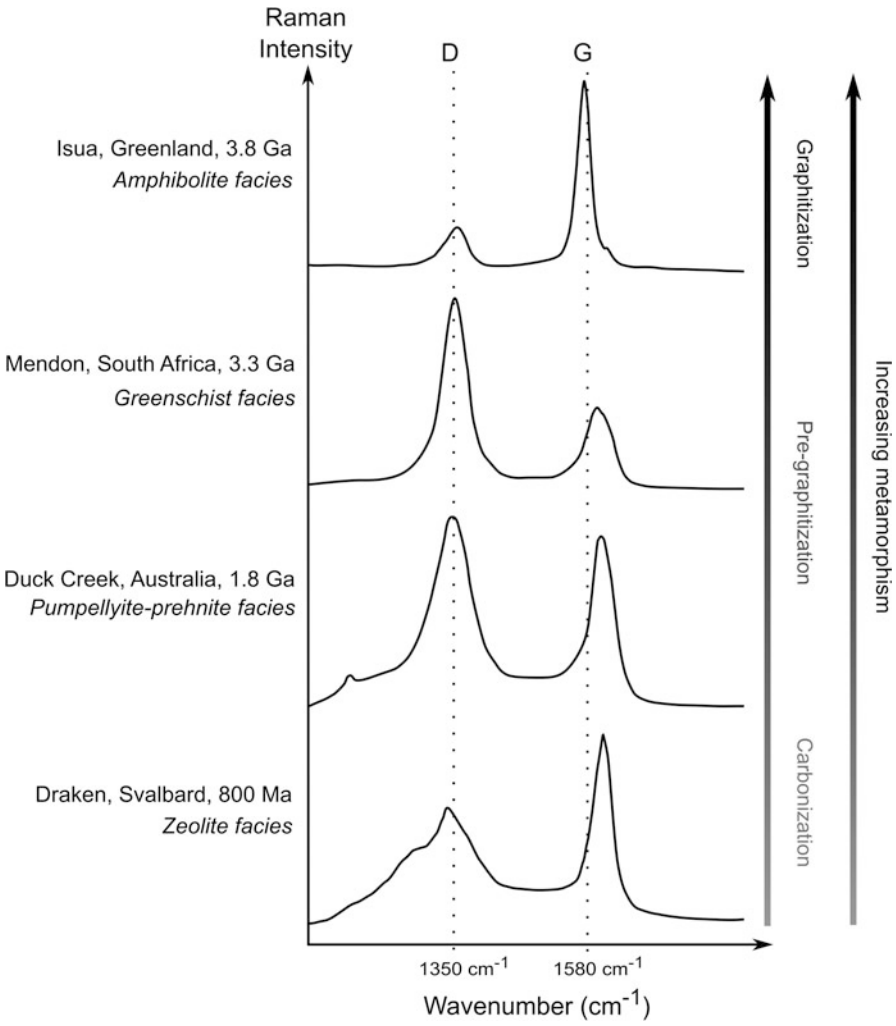

Fig. 13.5 Raman spectrum of kerogen with increasing metamorphism (temperature) obtained using a 532 nm excitation laser wavelength. Source: Adapted from Foucher et al. (2015)

On the other hand, the Raman mapping technique was recently used to demonstrate that, due to the variation of the molecular composition over a cell, and thus of the precursor of the carbonaceous matter, the spatial distribution of the changes in the D/G band intensity ratio follows the shape of the biotic structures (Foucher et al. 2015; Qu et al. 2015). By contrast, they are randomly distributed for abiotic structures, as shown in Fig. 13.6. These changes can be explained by the survival of particular functional groups in the kerogen associated with different parts of the fossil (Qu et al. 2015; Alleon et al. 2016).

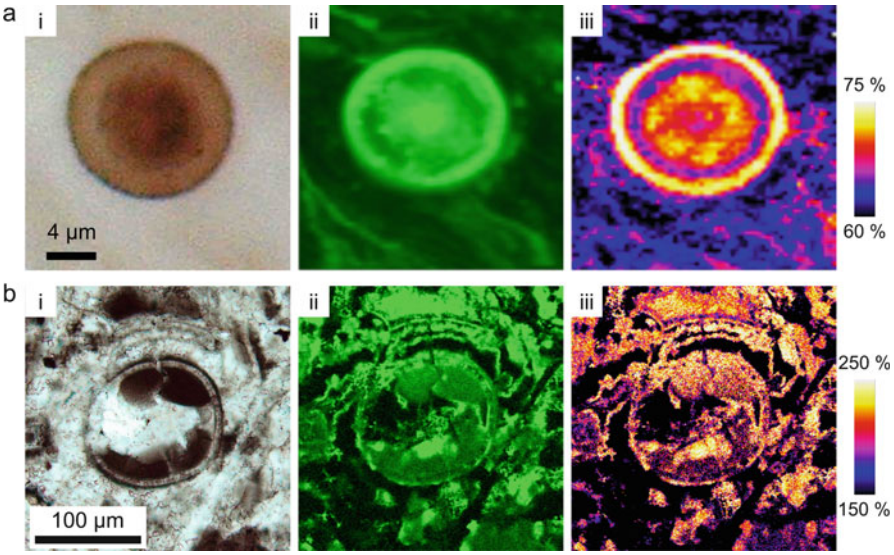

Fig. 13.6 Raman mapping of carbonaceous structures of (**a**-i, -ii, -iii) biotic and (**b**-i, -ii, -iii) abiotic origin. For each: (i) optical image, (ii) Raman map of carbonaceous matter and (iii) Raman map of the D/G peak intensity ratio obtained using a 532 nm excitation laser wavelength. Source: Adapted from Foucher et al. (2015)

13.3.4 Minerals and Microfossils

Although life is based on organic chemistry, it may also produce mineral compounds (biominerals, see Chap. 6). Large organisms biomediate the production of mineral components, such as bones, teeth or shells.

Microorganisms also produce minerals, either directly as a part of themselves, such as the frustules of diatoms, or indirectly as a result of their metabolic activities (precipitation of carbonates in the phototrophic layers forming stromatolites, for example). Contrary to organic matter that is rapidly recycled and reprocessed, mineral phases are less degraded with time making these types of biosignatures more susceptible to preservation on geological time scales and final detection in ancient sediments. On the other hand, most biominerals are known to be metastable, i.e. with metamorphism they tend to recrystallize into a more stable crystalline form. The same minerals can also form abiotically. Mineral structures must thus be placed in their mineralogical and environmental context to be considered as relevant biosignatures. Their shape (e.g. as a shell or stromatolite) and/or their association with carbonaceous matter are also very important (Rividi et al. 2010; Campbell et al. 2015).

Raman spectroscopy is particularly suited to study fossilized microorganisms since it is able to detect both carbonaceous matter and minerals at a (sub-)micrometre scale. Raman mapping is very powerful in its ability to display the relationships of mineral distributions in sediments with structures of biological origin. For instance, it has been shown that silicified carbonaceous microfossils in chert can be associated

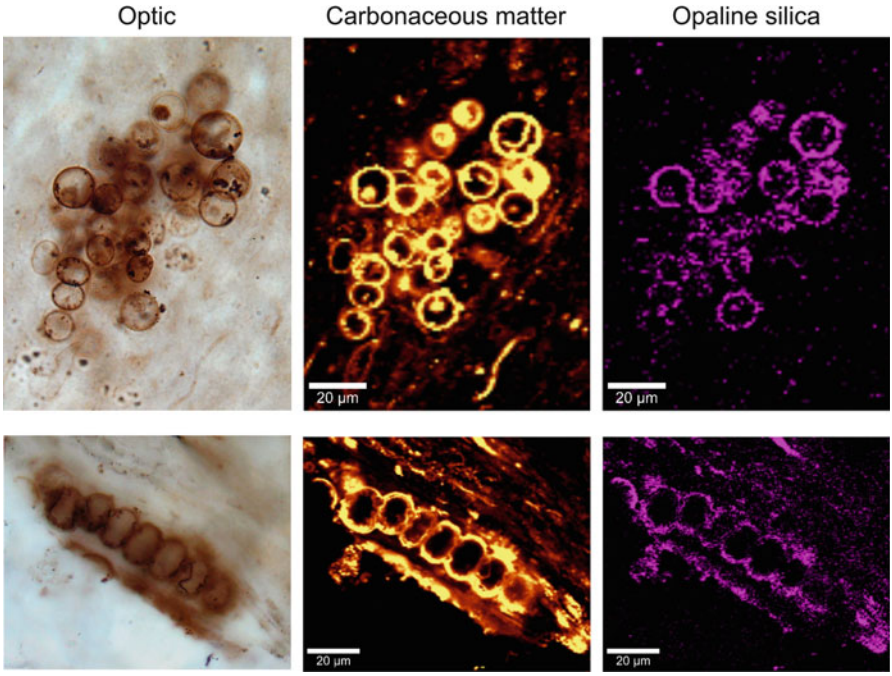

Fig. 13.7 Microfossils from the 800 Ma old Draken Formation (Svalbard) seen by optical microscopy in transmitted light, and associated Raman maps of carbonaceous matter and opaline silica obtained using a 532 nm excitation laser wavelength. Source: Adapted from Foucher and Westall (2013)

with amorphous silica despite the recrystallization of the silica matrix into quartz (Moreau and Sharp 2004) and this can be evidenced by Raman mapping, as shown in Fig. 13.7 (Foucher and Westall 2013). This interesting discovery is, however, limited to rocks of low grade metamorphism and requires the use of high resolution mapping techniques that are presently incompatible with space exploration.

13.3.5 Living Organisms

The holy grail of astrobiology remains the discovery of living extraterrestrial organisms and Raman spectroscopy could be particularly pertinent for this purpose. Among the techniques compatible with space exploration, it is one of the few capable of detecting living microorganisms at the surface of an extraterrestrial body without any sample preparation. The Raman spectrum of biological material consists of a superimposition of spectra of organic molecules, such as those described above in "organic molecules". Since biological materials are generally fluorescent, it is better

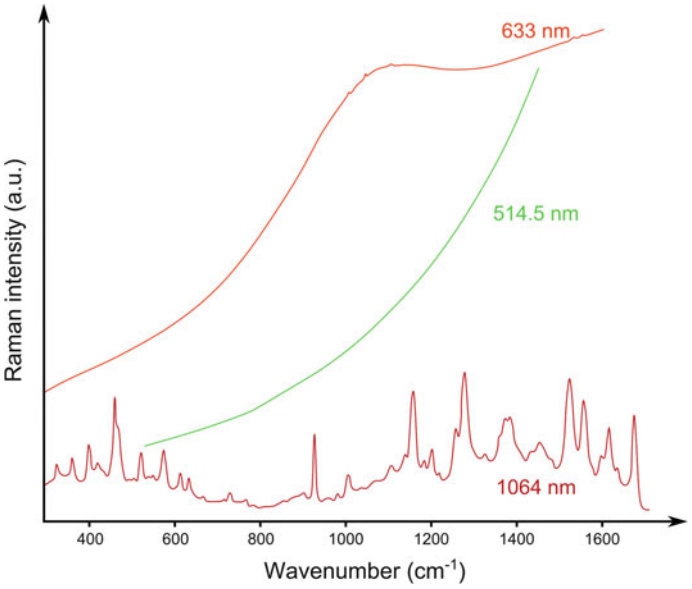

Fig. 13.8 Raman spectra of an Antarctic epilithic lichen, *Caloplaca saxicola*, from Beacon Sandstone, Mars Oasis, Antarctica, obtained using different laser wavelengths: 514.5, 633 and 785, and 1064 nm using FT Raman. Source: Adapted from Edwards (2004)

to use an IR excitation laser to detect living organisms, in particular in their natural environment as shown by Edwards (2004) (Fig. 13.8).

Observation of the Raman bands of organics in the range 400–1600 cm^{-1}, is generally difficult using a visible excitation laser, as displayed in Fig. 13.3. However, it is possible to detect the strong signal of CH and OH bands, in the 2800–3300 cm^{-1} and 3100–3650 cm^{-1} spectral regions, respectively, as well as the RR signal of pigments described above in "Pigments" (Edwards et al. 2013; Baqué et al. 2016; Jehlička et al. 2016).

13.4 Summary

Raman spectroscopy is particularly well-suited to the study of biosignatures, spanning a range from degraded biomolecules to living organisms. However, use of an inappropriate excitation laser wavelength may hamper the analyses. Most laboratory systems are equipped with several lasers, but this is not the case for the miniaturised system used for space exploration. In this case, the excitation wavelength must be chosen carefully in accordance with the aims of the analyses carried out and the corresponding targets (minerals, organics. . .). In any case, the high sensitivity of Raman spectrometers to carbonaceous matter will make it a key instrument for the detection of potential microfossils during the next *in situ* missions to Mars. In

addition, with its capacity to identify minerals and to detect pigments, we can count on this technique to make important discoveries in astrobiology and planetology in the coming decades.

Acknowledgements I thank the *Centre National d'Etudes Spatiales* for funding. I thank Frances Westall and Keyron Hickman-Lewis for their useful comments.

References

Alleon J, Bernard S, Guillou CL et al (2016) Molecular preservation of 1.88 Ga Gunflint organic microfossils as a function of temperature and mineralogy. Nat Commun 7:11977

Altwegg K, Balsiger H, Bar-Nun A et al (2016) Prebiotic chemicals-amino acid and phosphorus-in the coma of comet 67P/Churyumov-Gerasimenko. Sci Adv 2(e1600285):1–5

Baqué M, Verseux C, Böttger U et al (2016) Preservation of biomarkers from cyanobacteria mixed with mars like regolith under simulated Martian atmosphere and UV flux. Orig Life Evol Biosph 46:289–310

Beegle LW, Bhartia R, DeFlores L et al (2014) SHERLOC: scanning habitable environments with raman & luminescence for organics & chemicals, an investigation for 2020. In: 45th Lunar and planetary science conference, Abstract 2835

Beyssac O, Goffé B, Chopin C et al (2002) Raman spectra of carbonaceous material in metasidiments: a new geothermometer. J Metamorph Geol 20:859–871

Beyssac O, Goffé B, Petitet J-P et al (2003) On the characterization of disordered and heterogeneous carbonaceous materials by Raman spectroscopy. Spectrochim Acta Part A 59:2267–2276

Brack A (2001) Water the spring of life. In: Baumstark-Khan C, Horneck G (eds) Astrobiology: the quest for the conditions of life. Springer, New York, pp 79–88

Brasier MD, Green OR, Jephcoat AP et al (2002) Questioning the evidence for earth's oldest fossils. Nature 416:76–81

Bustin RM, Ross JV, Rouzaud JN (1995) Mechanisms of graphite formation from kerogen: experimental evidence. Int J Coal Geol 28:1–36

Campbell KA, Lynne BY, Handley KM et al (2015) Tracing biosignature preservation of geothermally silicified microbial textures into the geological record. Astrobiology 15:858–882

Culka A, Jehlička J, Vandenabeele P et al (2011) The detection of biomarkers in evaporite matrices using a portable Raman instrument under alpine conditions. Spectrochim Acta Part A 80:8–13

Culka A, Jehlička J, Strnad L (2012) Testing a portable Raman instrument: the detection of biomarkers in gypsum powdered matrix under gypsum crystals. Spectrochim Acta Part A 86:347–350

Danger G, Orthous-Daunay F-R, de Marcellus P et al (2013) Characterization of laboratory analogs of interstellar/cometary organic residues using very high resolution mass spectrometry. Geochim Cosmochim Acta 118:184–201

De Gelder J, Gussem KD, Vandenabeele P et al (2007) Reference database of Raman spectra of biological molecules. J Raman Spectrosc 38:1133–1147

de Marcellus P, Meinert C, Myrgorodska I et al (2015) Aldehydes and sugars from evolved precometary ice analogs: importance of ices in astrochemical and prebiotic evolution. Proc Natl Acad Sci USA 112(4):965–970

Deing T, Hollricher O, Toporski J (2010) Confocal Raman spectroscopy, Springer series in optical sciences 158. Heidelberg, Berlin

Deldicque D, Rouzaud JN, Velde B (2016) A Raman - HRTEM study of the carbonization of wood: a new Raman-based paleothermometer dedicated to archaeometry. Carbon 102:319–329

Dickens J, Irvine W, Nummelin A et al (2001) Searches for new interstellar molecules, including a tentative detection of aziridine and a possible detection of propenal. Spectrochimica Acta Part A 57:643–660

Dubessy J, Caumon MC, Rull F (2012) Raman spectroscopy applied to earth sciences and cultural heritage, EMU notes in mineralogy 12. The Mineralogical Society of Great Britain and Ireland
Edwards HGM (2004) Raman spetroscopic protocol for the molecular recognition of key biomarkers in astrobiological exploration. Orig Life Evol Biosph 34:3–11
Edwards HGM, Hutchinson I, Ingley R et al (2013) Raman spectroscopic analysis of geological and biogeological specimens of relevance to the ExoMars mission. Astrobiology 13:543–549
Ferrari AC (2007) Raman spectroscopy of graphene and graphite: disorder, electron–phonon coupling, doping and nonadiabatic effects. Solid State Commun 143:47–57
Foucher F, Westall F (2013) Raman imaging of metastable opal in carbonaceous microfossils of the 700–800Ma old draken formation. Astrobiology 13:57–67
Foucher F, Ammar MR, Westall F (2015) Revealing the biotic origin of silicified Precambrian carbonaceous microstructures using Raman spectroscopic mapping, a potential method for the detection of microfossils on Mars. J Raman Spectrosc 46:873–879
Foucher F, Guimbretière G, Bost N et al (2017) Petrographical and mineralogical applications of Raman mapping. In: Maaz K (ed) Raman spectroscopy and applications. IntechOpen, London, pp 163–180
Jehlička J, Bény C (1999) First and second order Raman spectra of natural highly carbonified organic compounds from metamorphic rocks. J Mol Struct 480–481:541–545
Jehlička J, Urban O, Pokorny J (2003) Raman spectroscopy of carbon and solid bitumens in sedimentary and metamorphic rocks. Spectrochim Acta Part A 59:2341–2352
Jehlička J, Edwards HGM, Vitek P (2009) Assessment of Raman spectroscopy as a tool for the non-destructive identification of organic minerals and biomolecules for Mars studies. Planet Space Sci 57:606–613
Jehlička J, Culka A, Nedbalova L (2016) Colonization of snow by microorganisms as revealed using miniature Raman spectrometers—possibilities for detecting carotenoids of psychrophiles on Mars? Astrobiology 16:913–924
Lahfid A, Beyssac O, Deville E et al (2010) Evolution of the Raman spectrum of carbonaceous material in low-grade metasediments of the Glarus Alps (Switzerland). Terra Nova 22:354–360
Lazcano A (2011) Origin of life. In: Gargaud M, Amils R, Cernicharo Quintanilla J et al (eds) Encyclopedia of astrobiology, vol 2. Springer, Heidelberg, pp 1183–1190
Lopez-Reyes G, Rull F, Venegas G et al (2013) Analysis of the scientific capabilities of the ExoMars Raman laser spectrometer instrument. Eur J Mineral 25:721–733
Marshall CP, Emry JR, Marshall AO (2011) Haematite pseudomicrofossils present in the 3.5-billion-year-old apex chert. Nat Geosci 4:240–243
Marshall AO, Emry JR, Marshall CP (2012) Multiple generations of carbon in the apex chert and implications for preservation of microfossils. Astrobiology 12:160–166
Marshall CP, Marshall AO (2013) Raman hyperspectral imaging of microfossils: potential pitfalls. Astrobiology 13:920–931
Meinert C, Myrgorodska I, de Marcellus P et al (2016) Ribose and related sugars from ultraviolet irradiation of interstellar ice analogs. Science 352:208–212
Merlin JC (1985) Resonance Raman spectroscopy of carotenoids and carotenoid containing systems. Pure Appl Chem 57:785–792
Moreau JW, Sharp TG (2004) A transmission electron microscopy study of silica and kerogen biosignatures in ~1.9 Ga gunflint microfossils. Astrobiology 4:196–210
Mosier-Boss P, Putnam MD (2013) The evaluation of two commercially available, portable Raman systems. Anal Chem Insights 8:83–97
Pasteris JD, Wopenka B (2002) Images of the earth's earliest fossils? Nature 420:476–477
Pasteris JD, Wopenka B (2003) Necessary, but not sufficient: Raman identification of disordered carbon as a signature of ancient life. Astrobiology 3:727–738
Patel M, Bérces A, Kerékgyarto T et al (2004) Annual solar UV exposure and biological effective dose rates on the Martian surface. Adv Space Res 33:1247–1252
Pflug HD, Jaeschke-Boyer H (1979) Combined structural and chemical analysis of 3.800-Myr-Old microfossils. Nature 280:483–486

Poilblanc R, Crasnier F (2006) Spectroscopies Infrarouge et Raman, Collection Grenoble Science (ed) EDP Sciences, Grenoble

Qu Y, Engdahl A, Zhu S et al (2015) Ultrastructural heterogeneity of carbonaceous material in ancient cherts: investigating biosignature origin and preservation. Astrobiology 15(10):825–842

Quirico E, Montagnac G, Rouzaud JN et al (2009) Precursor and metamorphic condition effects on Raman spectra of poorly ordered carbonaceous matter in chondrites and coals. Earth Planet Sci Lett 287:185–193

Rividi N, van Zuilen M, Philippot P et al (2010) Calibration of carbonate composition using micro-Raman analysis: application to planetary surface exploration. Astrobiology 10:293–309

Rouzaud JN, Oberlin A (1989) Structure, microtexture, and optical properties of anthracene and saccharose-based carbons. Cent Eur J Phys 27:517–529

Ruiz-Mirazo K, Moreno A (2011) Life. In: Gargaud M, Amils R, Cernicharo Quintanilla J et al (eds) Encyclopedia of astrobiology, vol 2. Springer, Heidelberg, pp 919–921

Rull-Pérez F, Martinez-Frias J (2006) Raman spectroscopy goes to Mars. Spectroscopy Europe 18:18–21

Schmitt-Kopplin P, Gabelica Z, Gougeon RD et al (2010) High molecular diversity of extraterrestrial organic matter in Murchison meteorite revealed 40 years after its fall. Proc Natl Acad Sci USA 7 (7):2763–2768

Schopf JW, Kudryavtsev AB, Agresti DG et al (2002a) Laser-Raman imagery of earth's earliest fossils. Nature 416:73–76

Schopf JW, Kudryavtsev AB, Agresti DG et al (2002b) Images of the earth's earliest fossils? Schopf et al reply. Nature 420:477

Schopf JW, Kudryavtsev AB, Agresti DG et al (2005) Raman imagery: a new approach to assess the geochemical maturity and biogenecity of permineralized precambrian fossils. Astrobiology 5:333–371

Sforna MC, van Zuilen MA, Philippot P (2014) Structural characterization by Raman hyperspectral mapping of organic carbon in the 3.46 billion-year-old apex chert, Western Australia. Geochim Cosmochim Acta 124:18–33

Vandenabeele P, Jehlička J, Vitek P, Edwards HGM (2012) On the definition of Raman spectroscopic detection limits for the analysis of biomarkers in solid matrices. Planet Space Sci 62:48–54

Vitek P, Osterrothova K, Jehlička J (2009) Beta-carotene - a possible biomarker in the Martian evaporitic environment: Raman micro-spectroscopic study. Planet Space Sci 57:454–459

Vitek P, Jehlička J, Edwards HGM et al (2012) The miniaturized Raman system and detection of traces of life in halite from the atacama desert: some considerations for the search for life signatures on Mars. Astrobiology 12:1095–1099